RESEARCH ARTICLE
DOI: 10.4274/tjh.galenos.2025.2024.0365

Identification of TRAPPC4 as a Key Autoantigen in Immune-Related Pancytopenia: Epitope Characterization and Immune Activation Mechanisms

Shanfeng Hao[1,2,3]*, Yang Zhang[1,2,3]*, Na Xiao[1], Zonghong Shao[1,2,3]
[1]Tianjin Medical University General Hospital, Department of Hematology, Tianjin, P. R. China
[2]Tianjin Key Laboratory of Bone Marrow Failure and Malignant Hemopoietic Clone Control, Tianjin, P. R. China
[3]Tianjin Institute of Hematology, Tianjin, P.R. China

***These authors contributed equally to this work.**

Zonghong Shao, M.D., Tianjin Medical University General Hospital, Department of Hematology; Tianjin Key Laboratory of Bone Marrow Failure and Malignant Hemopoietic Clone Control; Tianjin Institute of Hematology, Tianjin, P.R. China
szhong1235@163.com

September 28, 2024
January 16, 2025

Abstract

Objective: Immune-related pancytopenia (IRP) is characterized by autoantibody-mediated destruction or suppression of bone marrow cells, leading to pancytopenia. This study aimed to explore the role of TRAPPC4 (trafficking protein particle complex subunit 4) as a key autoantigen in IRP, including epitope identification and immune activation mechanisms.

Methods: A total of 90 participants were included in the study, divided into four groups: 30 newly diagnosed IRP patients, 25 IRP remission patients, 20 patients with control hematologic conditions (severe aplastic anemia [SAA] and myelodysplastic syndrome [MDS]), and 15 healthy controls. TRAPPC4 was identified using affinity screening with a phage random peptide library and confirmed with ELISPOT and epitope prediction software. TRAPPC4 expression in bone marrow cells and serum antibody titers was assessed via flow cytometry, ELISA, and real-time PCR. Immune cell profiling of peripheral blood

mononuclear cells (PBMNCs) was conducted using flow cytometry.
Results: TRAPPC4 was overexpressed on CD34+ bone marrow hematopoietic progenitor cells in newly diagnosed IRP patients compared to remission patients, disease controls (SAA and MDS), and healthy controls, with no significant differences observed in CD15+ granulocytes or CD235a+ nucleated red blood cells. The epitope peptide YTADGKEVLEYLG activated Th2 cells, as confirmed by ELISPOT. Newly diagnosed IRP patients exhibited elevated TRAPPC4 mRNA and protein levels in bone marrow mononuclear cells and higher serum antibody titers compared with controls. Immune profiling revealed increased CD19+ and CD5+CD19+ B lymphocytes in IRP patients.
Conclusion: TRAPPC4 was found as a key autoantigen in IRP, along with CD34+ cells as primary targets of autoantibody attacks. The identification of TRAPPC4 and its epitope provided insights into IRP pathogenesis and suggested potential diagnostic and therapeutic strategies.
Keywords: TRAPPC, cytopenia, autoantigen, autoantibody, immune-related

1 Introduction

Autoimmune diseases targeting the bone marrow, such as immune-related pancytopenia (IRP), lead to severe conditions like pancytopenia due to immune-mediated destruction of bone marrow cells. Despite advancements in research, the specific autoantigens involved in IRP remain unidentified, limiting the development of targeted therapies [1,2]. TRAPPC4 (trafficking protein particle complex subunit 4) has emerged as a potential autoantigen [3]. This protein, part of the TRAPP complex, is critical for intracellular transport within the Golgi apparatus, essential for hematopoietic cell function and bone marrow homeostasis [4]. Dysregulated TRAPPC4 has been linked to cancer, neurodegenerative disorders, and immune dysfunctions [5]. Autoantibodies targeting TRAPPC4 may impair its function, triggering cell dysfunction and destruction via complement activation or macrophage phagocytosis, potentially linked to Th2 cell imbalances [6,7].

Research conducted since 2000 identified TRAPPC4 as a candidate autoantigen in IRP through studies on patients with unexplained hemocytopenia and positive BMMNC-Coombs tests [8,9]. IRP pathogenesis involves T-lymphocyte dysregulation, increased Th2 cells, and elevated Th9 cells and IL-9, promoting autoantibody production [10-12]. TRAPPC4's role in vesicular trafficking, autophagy, and hematopoietic cell signaling, particularly through the ERK-MAPK pathway, highlights its potential involvement in IRP pathogenesis. Autoantibodies against TRAPPC4 may impair hematopoietic progenitor cell function, contributing to disease symptoms and serving as diagnostic markers.

This study aimed to investigate TRAPPC4's role in IRP and its correlation with disease severity. Identifying TRAPPC4 as a key autoantigen in IRP could enhance diagnostic precision and enable targeted therapies, improving patient outcomes and reducing side effects associated with broad immunosuppressive treatments.

2 Materials and methods

2.1 Patients

IRP is a hematologic condition caused by immune-mediated destruction or suppression of bone marrow hematopoietic cells, resulting in cytopenias across one or more blood cell lineages. Diagnosis is based on clinical, laboratory, and immunological findings, including evidence of autoantibodies or immune

abnormalities detected through assays. Criteria for IRP diagnosis included: (1) hemocytopenia or pancytopenia with normal or elevated reticulocyte/neutrophil percentages; (2) bone marrow showing normal or increased erythroid cells with visible erythroblastic islands; (3) exclusion of other primary/secondary hemocytopenia causes; and (4) positive BMMNC-Coombs test or autoantibodies on BM hematopoietic cells via flow cytometry (FCM). IRP was differentiated from severe aplastic anemia (SAA) and myelodysplastic syndrome (MDS) by the presence of erythroblastic islands (absent in SAA), lack of MDS-associated dysplastic changes, and immune markers unique to IRP. Other pancytopenia causes, including infections, nutritional deficiencies, and drug-induced cytopenias, were excluded through detailed clinical history, laboratory tests, and bone marrow evaluation to ensure diagnostic specificity.
Participants were divided into four groups: (1) Untreated IRP group (30 newly diagnosed, untreated patients), (2) Recovered IRP group (25 patients in remission or with significant improvement), (3) Disease control group (20 patients, including 10 with SAA and 10 with MDS, for comparative analysis), and (4) Healthy control group (15 age- and sex-matched individuals without hematologic disorders).
The inclusion of disease control groups helped distinguish IRP-specific immunologic features from conditions with overlapping clinical presentations. A total of 90 participants, all inpatients from February 2019 to May 2020, were enrolled, although sample availability affected assay counts. The study was approved by the Tianjin Medical University General Hospital ethics committee (Approval No. 20160301), and informed consent was obtained from all participants.

2.2 Screening TRAPPC4 Epitope and Synthesizing Antigen Peptide

Antibody Purification: Peripheral blood from 23 IRP patients and 10 healthy controls was processed to extract serum and antibodies via affinity chromatography.

Peptide Library Screening: A phage-display peptide library was used to identify TRAPPC4 epitopes bound by patient serum antibodies. Patient and control sera were coupled with magnetic beads and incubated with the library to isolate specific epitopes. Three rounds of screening with increasingly stringent washes were conducted to ensure specificity.

Positive Clone Identification and Sequencing: Positive phage clones were identified using ELISA, and sequences were determined after further amplification and purification.

2.3 Sterile Mononuclear Cell Culture

PBMCs were isolated from anticoagulated whole blood, cultured in a serum-supplemented medium, and prepared for downstream applications, including the IL4-ELISPOT assay.

2.4. IL4-ELISPOT

This assay evaluated IL-4 cytokine production in response to stimulation. Positive and negative control groups were included to establish assay sensitivity and background levels. The experimental group was stimulated with specific and negative control peptides. After incubation, cytokine spots were visualized and quantified.

2.5 Detection of TRAPPC mRNA levels by fluorescence quantitative polymerase chain reaction (FQ-PCR):

Total RNA was extracted using the TIANGEN RNAprep Pure Kit, which includes DNase treatment to remove genomic DNA and ensure RNA purity. Reverse transcription was carried out with the FastQuant RT kit, which uses both oligo(dT) and random primers for efficient cDNA synthesis. The QF-PCR was performed on a Bio-Rad iQ5 Real-Time system using SYBR Green dye to detect double-stranded DNA.

Primers for TRAPPC and GAPDH were synthesized by GENEWIZ. The PCR cycling program involved initial denaturation at 95°C, followed by 45 cycles of denaturation, annealing, and extension. TRAPPC mRNA levels were normalized to GAPDH and calculated using the $2^{-\Delta\Delta Ct}$ method.

2.6 Detection of TRAPPC4 Expression on Bone Marrow CD34+/CD235a+/CD15+ Cells by FCM:

1. FCM detected TRAPPC4 expression in CD34+, CD235a+, and CD15+ bone marrow cells. Control tubes (negative and isotype) and experimental tubes were prepared. Cells were stained with antibodies, processed with hemolysin, washed, and analyzed using CytoExpert software. Gating strategies ensured accurate cell population identification.

2.7 Determination of CD5+ B Lymphocyte Ratio

1. The proportion of CD5+ B lymphocytes in bone marrow CD19+ cells was determined using FCM. Antibody-labeled samples were incubated, treated with lysate, and analyzed for co-expression of CD19 and CD5 markers.

2.8 Western blotting used for detection of TRAPPC4 protein level in BMMNCs

Bone marrow samples were collected with heparin as an anticoagulant, and BMMNCs were isolated using density gradient centrifugation. Proteins were extracted by lysing cells with RIPA buffer containing protease inhibitors, and their concentration was measured using the BCA protein assay, a colorimetric method detecting protein concentration via absorbance at 562 nm. Equal protein amounts (20–30 μg) were separated by SDS-PAGE, transferred onto PVDF membranes, blocked with 5% milk in TBS-T, and incubated with primary antibodies against TRAPPC4 and GAPDH (loading control) overnight at 4°C. After washing, membranes were incubated with HRP-conjugated secondary antibodies, and protein detection was performed using the ECL method. Signals were visualized with an imaging system, and band intensity was analyzed using ImageJ software. TRAPPC4 protein levels were normalized to GAPDH for comparative analysis.

2.9 Detection of Serum TRAPPC4 Concentration by ELISA

Serum TRAPPC4 levels were measured in 22 untreated IRP patients, 14 recovered IRP patients, and 5 healthy controls, determined by available samples. Blood samples (2 mL each) were collected, centrifuged at 3000 rpm for 10 minutes, and the supernatants stored at -80°C for analysis. TRAPPC4 quantification employed an ELISA kit with a stepwise procedure: plate washing, standard/sample addition, incubation, biotin-labeled antibody addition, and further incubation with SABC solution. Following substrate addition and reaction termination, absorbance was measured using a plate reader.

2.10 Expression and purification of the recombinant TRAPPC proteins

TRAPPC4 gene amplification used specific primers based on cDNA sequences. PCR products were inserted into the pEASY™-E1 vector and transformed into *E. coli* Trans1-T1 cells. Positive clones were confirmed via colony PCR and sequencing. For protein expression, plasmids were transformed into *E. coli* BL21 cells, with IPTG induction at 1 mM. Cells were lysed, and proteins were purified using Ni-NTA affinity chromatography. Eluted proteins were analyzed by SDS-PAGE and Coomassie staining for purity, validated by Western blotting. Refolding of purified proteins was performed in a urea gradient buffer at 4°C for 12 hours per gradient step. Final protein concentrations were measured using the BCA assay.

2.11 Detection of TRAPPC4 Antibody in Bone Marrow Supernatant by ELISA

Bone marrow supernatants were analyzed using an ELISA protocol. Plates were coated with TRAPPC4 protein (2 μg/mL), incubated at 4°C overnight, washed with PBST, and blocked with 2% BSA. Diluted

serum samples (1:100) were added, incubated at 37°C for 1.5 hours, and detected with a secondary antibody (1:2500) and TMB substrate. After stopping the reaction, absorbance was measured. The binding index (BI) was calculated using the formula:

BI = (OD sample - OD blank) / (OD control - OD blank)

where, OD control represents the absorbance of mixed serum from eight randomly selected samples, and OD blank corresponds to the absorbance of the blank control well.

2.12 Statistical Analysis

Statistical analysis was conducted using SPSS 24.0 software, with normally distributed data expressed as mean ± standard deviation. A t-test was used for two-group comparisons, with $P < 0.05$ considered statistically significant. Graphs and figures were created using GraphPad Prism 8.0 software.

3 Results

3.1 Screening TRAPPC4 epitope and synthesis of antigen peptide

Antibodies were obtained from eluents of 10 normal and 23 IRP-mixed serum samples after protein G purification. Following three rounds of screening, eluting phage titers increased, indicating enrichment. ELISA was used for detection, and 10 clones were selected based on recognition by patient antibodies but not by normal antibodies. These clones were sequenced, revealing four peptides: WSLGYTG, TIYTTWQ, WSLGYTR, and YTTTLTY. These peptides contained the YT sequence, with two also containing LG. Alignment with TRAPPC4's amino acid sequence highlighted the YTADGKEVLEYLG peptide, suggesting it could be an antigenic epitope. Further analysis using IEDB predicted antigenic binding to MHC-II, identifying YTADGKEVLEYLGNP as a positive peptide and LALEVAEKAGTFGPG as a negative peptide.

3.2 Verifying the effect of antigen peptides on Th2 cells using IL4-ELISPOT

The positive peptide YTADGKEVLEYLGNP significantly stimulated IL-4 production in newly diagnosed IRP patients, whereas the negative peptide LALEVAEKAGTFGPG did not result in a significant increase in IL-4 production (Figure 1).

3.3 Detection of TRAPPC4 expression in bone marrow CD34+/CD235a+/CD15+ cells by FCM

FCM analysis showed varying TRAPPC4 expression levels across cell types and patient groups, reported as percentages of positive cells. TRAPPC4 expression was significantly higher in CD34+ cells from the untreated IRP group (11.74±2.16%) compared to the recovered IRP group (1.01±1.18%), case-control group (5.24±3.69%), and normal control group (0.63±0.91%) ($P < 0.05$). However, no significant differences were observed in TRAPPC4 expression on CD15+ or CD235a+ cells across the groups ($P = 0.15$ and $P = 0.17$, respectively). Additionally, no increase in TRAPPC4 positivity was found in CD235a+ nucleated red blood cells ($P = 0.23$), suggesting TRAPPC4 dysregulation may be more relevant to early-stage hematopoietic progenitor cells, such as CD34+ cells, rather than terminally differentiated erythroid cells.

3.4 Detection of serum TRAPPC4 concentration by ELISA

Serum TRAPPC4 levels were significantly higher in untreated IRP patients (0.87±0.44, n=22) compared with recovered IRP patients (0.51±0.41, n=14) and normal controls (0.41±0.33, n=5) ($P < 0.05$). No significant difference was observed between recovered IRP patients and normal controls ($P = 0.19$).

3.5 Detection of TRAPPC4 mRNA expression by FQ-PCR

TRAPPC4 mRNA expression was also significantly elevated in untreated IRP patients (0.79±0.87, n=15) compared to recovered IRP patients (0.42±0.44, n=25) and normal controls (0.22±0.22, n=17) ($P<0.05$). Additionally, recovered IRP patients exhibited significantly higher TRAPPC4 mRNA levels than normal controls ($P < 0.05$).

3.6 Detection of TRAPPC4 protein in bone marrow mononuclear cells (BMMNC) by Western blotting

Western blot analysis demonstrated that the expression level of TRAPPC4 in untreated IRP patients was significantly higher than that in recovered IRP patients and normal controls ($P < 0.05$, Figure 2A).

3.7 Detection of B cells and CD5+ B cells by FCM

The proportion of CD19+ cells in PBMNCs was higher in the IRP untreated group (11.72±7.79%) compared to the IRP recovered group (7.64±5.54%), MDS group (9.89±6.26%), and SAA group (10.43±7.48%). A statistically significant difference was found only between the IRP untreated and IRP recovered groups ($P = 0.0033$). Similarly, the proportion of CD5+ CD19+/CD19+ cells was higher in the IRP untreated group (2.23±2.39%) than in the other groups, with significant differences observed only between the IRP untreated and recovered groups ($P = 0.0063$). The proportion of CD5+ CD19+/PBMNCs was also higher in the IRP untreated group (0.35±0.48%) compared to the others, with a significant difference only between the IRP untreated and recovered groups ($P = 0.0050$). No significant differences were found between the other groups. Supplementary Figure 1 shows FCM results comparing IRP patients and healthy controls.

3.8 Expression and purification of TRAPPC4 protein

The TRAPPC4 gene was amplified by PCR and inserted into the Peasy-E1 vector. Recombinant plasmids were transformed into *E. coli* BL-21, identified by PCR and sequencing, and induced for expression using IPTG. Fusion proteins were expressed, confirmed by Western blot with an anti-histidine antibody, and purified with ProteinIso Ni-NTA Resin. The optimal imidazole elution concentration for TRAPPC4 protein was 500 mM. The protein was renatured by dialysis, and its concentration, measured using the BCA method, was 622.5 μg/mL (Figures 3 and 4).

3.9 Detection of TRAPPC4 antibody levels in the bone marrow supernatant of patients with IRP by ELISA

The levels of anti-TRAPPC antibodies in the serum of untreated IRP patients (1.35±0.31 AU) were significantly higher compared to those in recovered IRP patients (1.18±0.32 AU) and normal controls (1.12±0.21 AU), and the differences were statistically significant ($P < 0.05$). However, there were no significant differences in anti-TRAPPC antibody levels between recovered IRP patients and normal controls ($P > 0.05$) (Figure 2B).

3.10 Linking TRAPPC4 expression to IRP pathogenesis

Elevated TRAPPC4 expression at the mRNA and protein levels in untreated IRP patients, along with increased anti-TRAPPC4 antibody production, suggests its role as an autoantigen in autoimmune responses. TRAPPC4 could contribute to Th2 cell activation and IL-4 production, as evidenced by ELISPOT assay. These findings position TRAPPC4 as a key molecular target, providing insights into the autoimmune mechanisms of IRP and warranting further investigation into its role in disease progression.

4 Discussion:

This study identified trafficking protein particle complex subunit 4 (TRAPPC4) as a potential autoantigen

in IRP. Elevated TRAPPC4 expression was observed in bone marrow hematopoietic progenitor cells, serum, and mononuclear cells of IRP patients compared to controls. TRAPPC4-specific antibodies and the YTADGKEVLEYLG peptide epitope were shown to activate Th2 cells, confirming its immunogenicity and involvement in IRP pathogenesis through autoantibody-mediated immune disruption [7,9,14].

IRP, an autoimmune-related form of idiopathic cytopenia of uncertain significance (ICUS) [13–15], involves autoantibodies targeting CD34+ hematopoietic progenitor cells. Flow cytometry revealed increased TRAPPC4 expression on these cells in newly diagnosed IRP patients compared to remission and control groups, implicating early hematopoietic cells as primary targets [16,17]. Higher TRAPPC4 mRNA and protein levels in BMMNCs and elevated TRAPPC4-specific antibody titers in IRP patient serum further support its pathogenic role. However, no significant increase was noted in CD235a+ nucleated red blood cells, suggesting a focus on early progenitor cells.

TRAPPC4, a core subunit of the TRAPP complex, is critical for intracellular transport, autophagy, and signaling pathways such as ERK-MAPK. Its dysregulation in IRP may impair autophagy, disrupt vesicular trafficking, and promote apoptosis in hematopoietic progenitors. The abnormal membrane localization of TRAPPC4 in IRP patients likely renders it immunogenic, leading to autoimmune responses [5,7,11,16].

Despite promising findings, the study's limitations include its cross-sectional design, small sample size, and lack of mechanistic validation. Future studies should utilize animal models, proteomic analyses, and single-cell RNA sequencing to explore TRAPPC4 regulation and its role in IRP pathogenesis.

Abbreviations

IRP: Immune-related pancytopenia
BMMNC: bone marrow mononuclear cells
BM: bone marrow
FCM: flow cytometry
SDS-PAGE: sodium dodecyl sulfate-polyacrylamide gel electrophoresis
ICUS: idiopathic cytopenia of uncertain significance
MDS: myelodysplastic syndrome
AA: aplastic anemia

Acknowledgements

Not applicable.

Author contributions

Zonghong Shao: Conceptualization, Methodology, Resources, Supervision, Funding acquisition, Writing – review & editing.
Shanfeng Hao: Validation, Writing – original draft, Formal analysis.
Yang Zhang: Validation, Writing – review & editing.
Na Xiao: Investigation.
All the authors read and approved the final manuscript.

Availability of data and materials

The dataset generated and analysed during the current study is available in the supplementary files.

Ethics approval and consent to participate

The research protocol was approved by the ethics committee of Tianjin Medical University General Hospital (No. 20160301). All patients provided informed consent before participating in the trial.

Patient consent for publication

Not applicable.

Competing interests

The authors declare that there is no conflict of interest.

Funding

This research was supported by the National Natural Science Foundation of China (No. 81600088 and No. 81770118).

References

1. Park M. Overview of inherited bone marrow failure syndromes. Blood Res. 2022;57(S1):49-54.
2. Xiao N, Hao S, Zhang Y, et al. Roles of immune responses in the pathogenesis of immunorelated pancytopenia. Scand J Immunol. 2020;92(2):e12911.
3. Ren Y, Qian Y, Ai L, et al. TRAPPC4 regulates the intracellular trafficking of PD-L1 and antitumor immunity. Nat Commun. 2021;12(1):5405.
4. He H, Shao Z, Liu H, et al. Immunorelated pancytopenia. Zhonghua Xue Ye Xue Za Zhi. 2021;22(2):79-82 (in Chinese).
5. Uehara J, Yoshino K, Sugiyama E, et al. Immune-related pancytopenia caused by nivolumab and ipilimumab combination therapy for unresectable melanoma of unknown primary. J Dermatol. 2020;47(6):e237-e239.
6. Kumar S, Jeong Y, Ashraf MU, et al. Dendritic Cell-Mediated Th2 Immunity and Immune Disorders. Int J Mol Sci. 2019;20(9):2159.
7. Shao Q, Wang Y, Liu Z, et al. Th9 Cells in Peripheral Blood Increased in Patients with Immune-Related Pancytopenia. J Immunol Res. 2020;6503539.
8. Groarke EM, Feng X, Aggarwal N, et al. Efficacy of JAK1/2 inhibition in murine immune bone marrow failure. Blood. 2023;141(1):72-89.
9. Li W, Wang F, Guo R, et al. Targeting macrophages in hematological malignancies: recent advances and future directions. J Hematol Oncol. 2022;15(1):110.
10. Cedzyński M, Thielens NM, Mollnes TE, et al. Editorial: The Role of Complement in Health and Disease. Front Immunol. 2019;10:1869.
11. Yu X, Wax J, Riemekasten G, et al. Functional autoantibodies: Definition, mechanisms, origin and contributions to autoimmune and non-autoimmune disorders. Autoimmun Rev. 2023;22(9):103386.
12. Littleton E, Dreger M, Palace J, et al. Immunocapture and identification of cell membrane protein antigenic targets of serum autoantibodies. Mol Cell Proteomics. 2009;8(7):1688-96.
13. El Jamal, S. M., Najfeld, V., Coltoff, A., & Navada, S. Myelodysplastic Syndromes. In Atlas

Diagn Hematol. 2020.
14. Saygin C, & Godley LA. Genetics of myelodysplastic syndromes. Cancers. 2021;13(14).
15. Shin DY, Park JK, Li CC, Park HS, Moon SY, Kim SM, Im K, Chang YH, Yoon SS, & Lee DS. Replicative senescence of hematopoietic cells in patients with idiopathic cytopenia of undetermined significance. Leuk. Res. 2019:79.
16. Goto M, Kuribayashi K, Takahashi Y, Kondoh T, Tanaka M, Kobayashi D, & Watanabe N. Identification of autoantibodies expressed in acquired aplastic anaemia. Br. J. Haematol. 2013:160(3).
17. Kelkka T, Tyster M, Lundgren S, Feng X, Kerr C, Hosokawa K, Huuhtanen J, Keränen M, Patel B, Kawakami T, Maeda Y, Nieminen O, Kasanen T, Aronen P, Yadav B, Rajala H, Nakazawa H, Jaatinen T, Hellström-Lindberg E. Anti-COX-2 autoantibody is a novel biomarker of immune aplastic anemia. Leuk. 2022;36(9).

Figure 1. IL-4 ELISPOT analysis. The number of spots in experimental group 2 (PBMCs + peptide 2) was significantly higher than that in the negative control well. However, there was no difference in the number of spots in experimental group 1 (PBMCs + peptide1) compared with the negative control well.

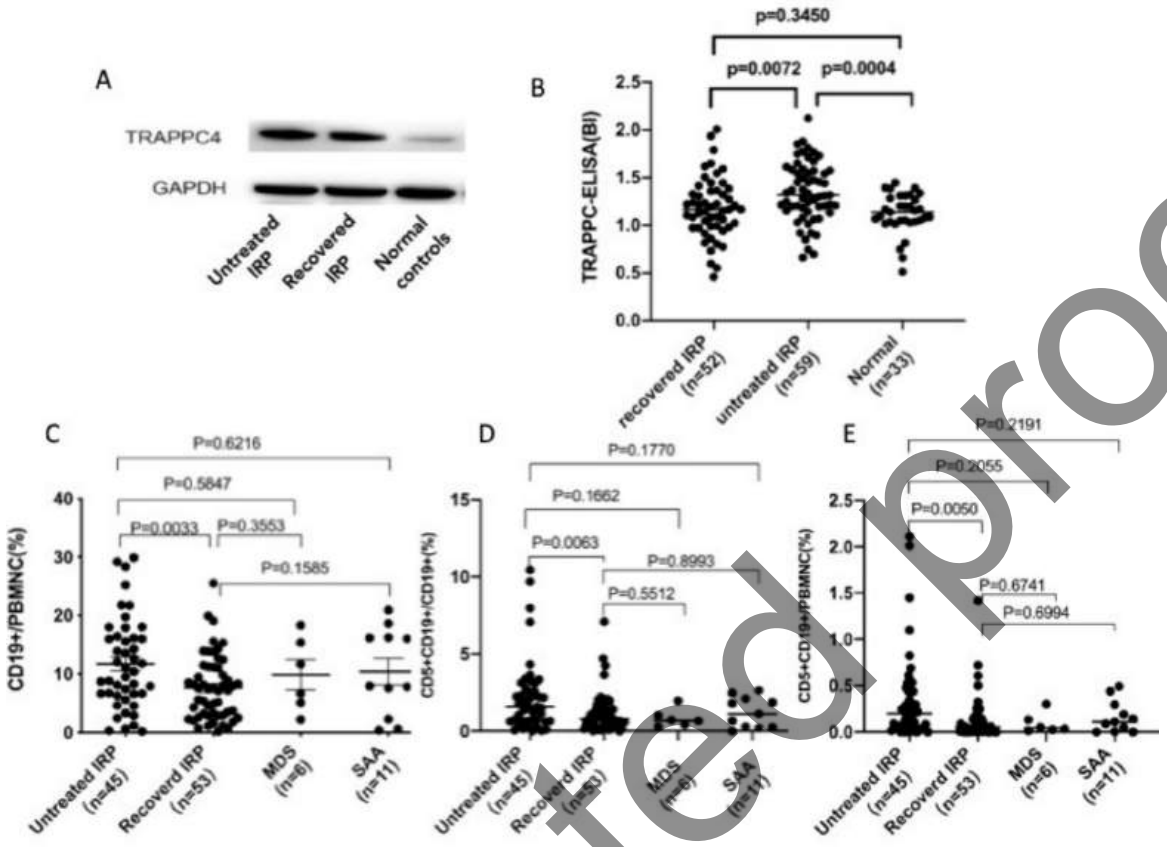

Figure 2. (A) TRAPPC4 protein level in BMMNC detected with Western blot. (B) The anti-TRAPPC antibodies levels in the serum of untreated IRP patients were significantly higher compared with the recovered IRP patients and normal controls. (C) The proportion of CD19+/PBMNC was higher in the IRP untreated group compared to the other groups. (D) The proportion of CD5 + CD19 + /CD19+ was higher in the IRP untreated group than that in the other groups. (E) The proportion of CD5 + CD19 + / PBMNC was higher in the IRP untreated group than that in the other groups.

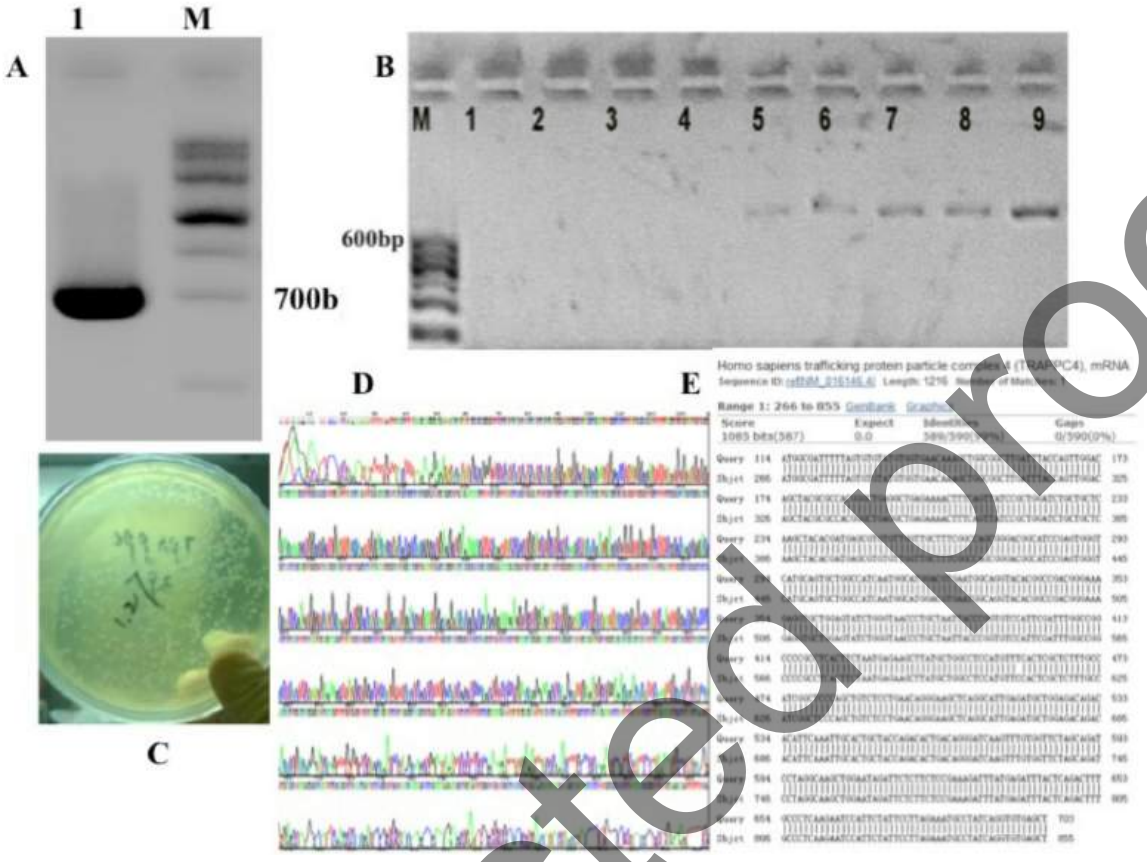

Figure 3. PCR amplification and cloning of TRAPPC4. (A) AGE result of the ORF encoding TRAPPC amplified from the pTriIEx2-FTL plasmid. lane marker: TIANGEN marker I; lane 1: ORF of TRAPPC4. (C) Competent E. coli Trans1-T1 colonies transformed with the ligated mixture of TRAPPC4 PCR products and the expression vector pEASYTM-E1. (B) Lane 1-9 showed the AGE result of PCR amplification of the 8 colonies randomly picked up from the plate with the vector primer T7-F and the primer TRAPPC4-R，lane 5-9 showed the forward positive clones. (D) Sequencing of the plasmid DNA extracted from the forward positive clones with T7 promoter and T7 terminator primer. (E) BLAST result showed DNA sequences coincided with the ORF of TRAPPC4 completely.

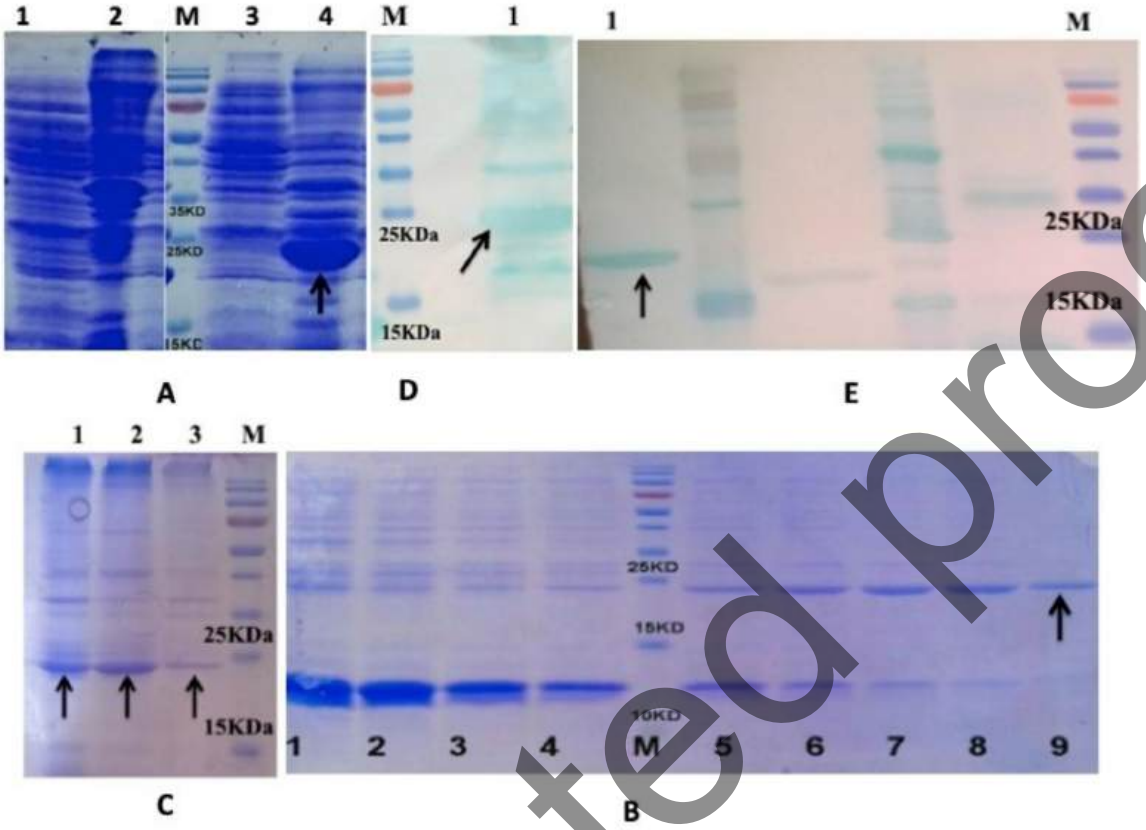

Figure 4. Expression and purification of TRAPPC4. (A) SDS-PAGE analysis of the pEASY-E1 in E.coli BL21 (DE3) cells and the pEASY-E1-TRAPPC in E.coli BL21(DE3) cells. Lane M: protein molecular marker; lane 1: The supernatant of empty pEASY-E1 in E.coli BL21(DE3) cells; lane 2: The precipitation of empty pEASY-E1 in E.coli BL21(DE3) cells; lane 3: The supernatant of pEASY-E1-TRAPPC4 in E.coli BL21(DE3) cells; lane 4: The precipitation of pEASY-E1-TRAPPC4 in E.coli BL21(DE3) cells. Recombinant TRAPPC4 (rTRAPPC4) was expressed as insoluble proteins and accumulated in inclusion bodies. It had a distinct band with molecular weight of about 21.5kDa (black arrow). (B) SDS-PAGE analysis of purified rTRAPPC4 eluted with different concentration of imidazole. Lane M: protein molecular marker; lane1-9: purified rTRAPPC4 eluted with 40,62.5,80,100,125,160,200,250 and 500 mM of imidazole in equilibration buffer (pH 8.0) respectively. Purified rTRAPPC4 eluted with 500 mM of imidazole (lane 9, black arrow) had relatively higher purity compared with others and 500 mM was identified as the optimum concentration. (C) SDS-PAGE analysis of purified rTRAPPC4. A total of three purified TRAPPC samples were initially loaded (lanes 1 and 3), and sample 2 is the one that was ultimately selected for subsequent experiments, due to its relatively higher purity, compared with samples 1 and 3 (the black arrow points to the target protein rTRAPPC4). (D) WB analysis of recombinant HIS-TRAPPC protein before purification (black arrow). (E) WB analysis of purified recombinant HIS-TRAPPC4 protein (lane 1, black arrow). The other two proteins loaded in other lanes are not relevant to the present study.

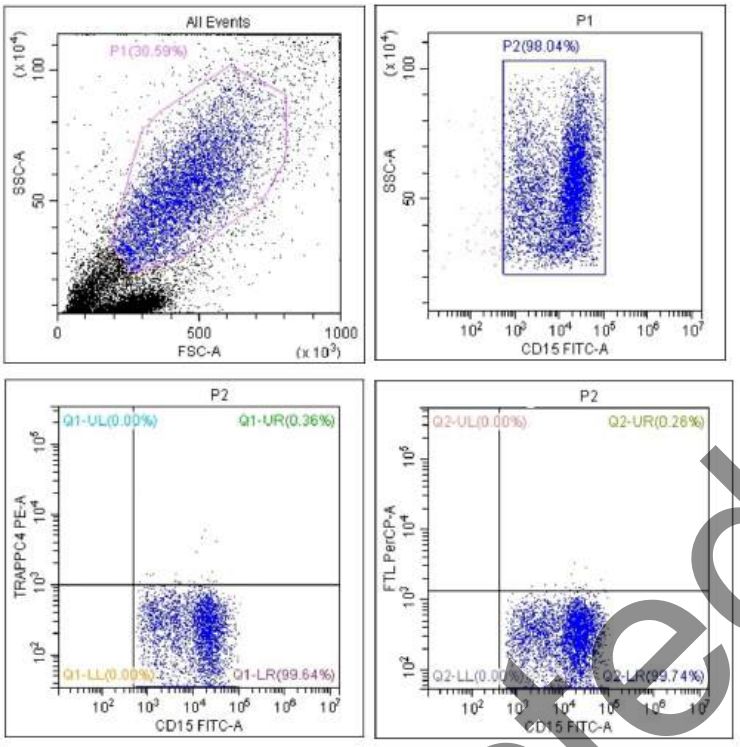

Supplementary Figure 1: Illustrating FCM results between IRP patients and healthy controls.

Figure S1a: CD15 Control

Panel A (Top Left): FSC-A vs. SSC-A (All Events): This scatter plot shows the distribution of all events based on forward scatter (FSC-A) and side scatter (SSC-A), which represent cell size and granularity, respectively. The gated population, labeled "P1," which accounts for 30.59% of the total events, is shown

within a magenta contour.

Panel B (Top Right): CD15 FITC-A vs. SSC-A (P1 Gated): After gating on the P1 population, this plot shows CD15 expression (FITC-A) on the x-axis versus side scatter (SSC-A) on the y-axis. A rectangular gate, labeled "P2" (98.04%), isolates the population of CD15-positive cells.

Panel C (Bottom Left): CD15 FITC-A vs. TRAPPC4 PE-A (P2 Gated): This plot presents CD15 expression (FITC-A) against TRAPPC4 fluorescence (PE-A) for the P2 gated population. Events are quadranted to identify distinct populations. Q1-LR (99.64%) represents cells that are CD15-positive and TRAPPC4-negative, while Q1-UR (0.36%) corresponds to a small subset of cells co-expressing both markers.

Panel D (Bottom Right): CD15 FITC-A vs. FTL PerCP-A (P2 Gated): In this plot, CD15 expression (FITC-A) is shown against FTL fluorescence (PerCP-A) for the P2 gated population. The majority of events fall in Q2-LR (99.74%), which corresponds to cells that are CD15-positive and FTL-negative. A small population (Q2-UR, 0.26%) represents cells that co-express both markers.

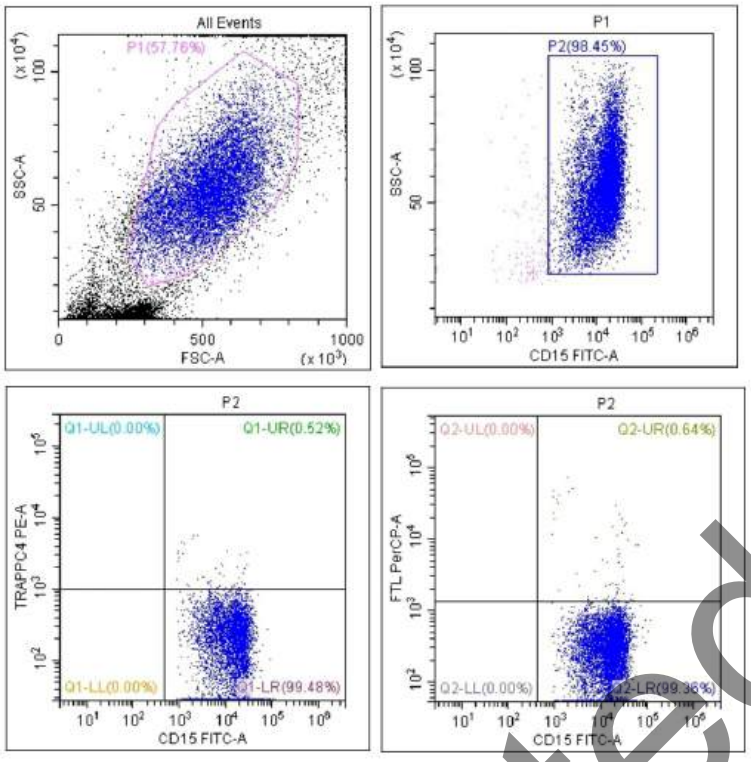

Figure S1b: CD15 IRP

Panel A (Top Left): FSC-A vs. SSC-A (All Events): This scatter plot shows the distribution of all events based on forward scatter (FSC-A) and side scatter (SSC-A), indicating cell size and granularity. The gated population, labeled "P1," comprises 57.76% of the total events.

Panel B (Top Right): CD15 FITC-A vs. SSC-A (P1 Gated): This plot shows CD15 expression (FITC-A) on the x-axis versus side scatter (SSC-A) on the y-axis for the P1 gated population. The gate "P2" (98.45%) isolates the CD15-positive population.

Panel C (Bottom Left): CD15 FITC-A vs. TRAPPC4 PE-A (P2 Gated): This plot presents CD15 expression (FITC-A) against TRAPPC4 fluorescence (PE-A) for the P2 gated population. Quadrant analysis shows Q1-LR (99.48%) with high CD15 and low TRAPPC4 expression, and Q1-UR (0.52%) as a minor population expressing both markers.

Panel D (Bottom Right): CD15 FITC-A vs. FTL PerCP-A (P2 Gated): In this plot, CD15 expression (FITC-A) is shown against FTL fluorescence (PerCP-A) for the P2 gated population. The majority of events fall in Q2-LR (99.36%) with high CD15 and low FTL expression, while Q2-UR (0.64%) represents a small population co-expressing both markers.

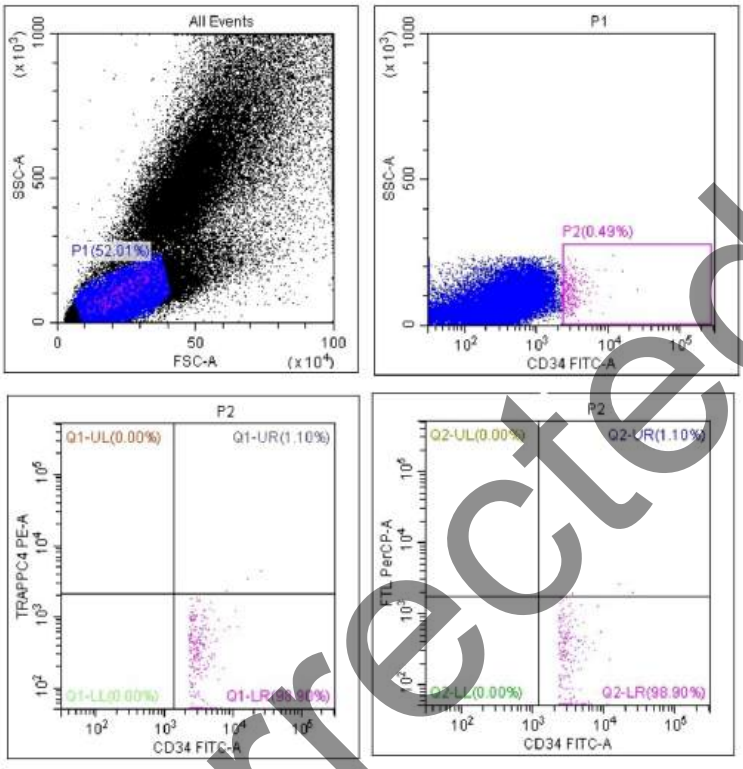

Figure Legend for S1c: CD34 Control

Panel A (Top Left): FSC-A vs. SSC-A (All Events): This scatter plot shows the distribution of all events based on forward scatter (FSC-A) and side scatter (SSC-A), indicating cell size and granularity. The gated population "P1" (52.01%) is highlighted within the magenta contour.

Panel B (Top Right): CD34 FITC-A vs. SSC-A (P1 Gated): This plot shows CD34 expression (FITC-A) on the x-axis versus side scatter (SSC-A) on the y-axis for the P1 gated population. The "P2" gate (0.49%) isolates CD34-positive cells.

Panel C (Bottom Left): CD34 FITC-A vs. TRAPPC4 PE-A (P2 Gated): This plot presents CD34 expression (FITC-A) on the x-axis and TRAPPC4 fluorescence (PE-A) on the y-axis for the P2 gated population. Quadrant analysis shows that Q1-LR (98.90%) represents cells that are CD34-positive and TRAPPC4-negative, while Q1-UR (1.10%) represents a small co-expressing population.

Panel D (Bottom Right): CD34 FITC-A vs. FTL PerCP-A (P2 Gated): This plot shows CD34 expression (FITC-A) against FTL fluorescence (PerCP-A) for the P2 gated population. The majority of events fall in Q2-LR (98.90%) with high CD34 and low FTL expression, and Q2-UR (1.10%) indicates a minor population co-expressing both markers.

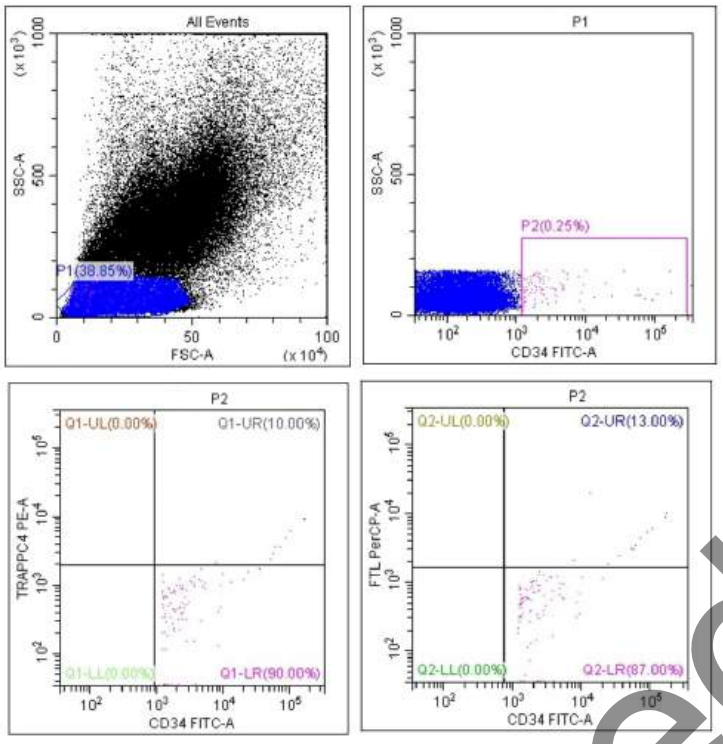

Figure S1d: CD34 IRP

Panel A (Top Left): FSC-A vs. SSC-A (All Events): This scatter plot shows the distribution of all events based on forward scatter (FSC-A) and side scatter (SSC-A), indicating cell size and granularity. The gated population, labeled "P1," comprises 38.85% of the total events.

Panel B (Top Right): CD34 FITC-A vs. SSC-A (P1 Gated): This plot shows CD34 expression (FITC-A) on the x-axis versus side scatter (SSC-A) on the y-axis for the P1 gated population. The gate "P2" (0.25%) isolates the CD34-positive population.

Panel C (Bottom Left): CD34 FITC-A vs. TRAPPC4 PE-A (P2 Gated): This plot presents CD34 expression

(FITC-A) against TRAPPC4 fluorescence (PE-A) for the P2 gated population. Quadrant analysis shows Q1-LR (90.00%) with high CD34 and low TRAPPC4 expression, and Q1-UR (10.00%) as a minor population expressing both markers.

Panel D (Bottom Right): CD34 FITC-A vs. FTL PerCP-A (P2 Gated): In this plot, CD34 expression (FITC-A) is shown against FTL fluorescence (PerCP-A) for the P2 gated population. The majority of events fall in Q2-LR (87.00%) with high CD34 and low FTL expression, while Q2-UR (13.00%) represents a small population co-expressing both markers.

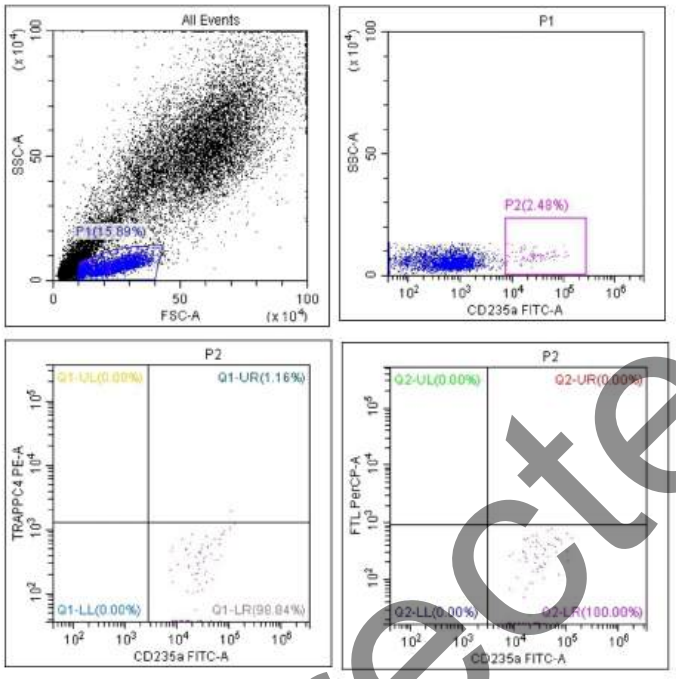

Figure S1e: CD235 Control

Panel A (Top Left): FSC-A vs. SSC-A (All Events): This scatter plot shows the distribution of all events

based on forward scatter (FSC-A) and side scatter (SSC-A), which represent cell size and granularity, respectively. The gated population, labeled "P1," which accounts for 15.89% of the total events, is shown within a magenta contour.

Panel B (Top Right): CD235 FITC-A vs. SSC-A (P1 Gated): After gating on the P1 population, this plot shows CD235 expression (FITC-A) on the x-axis versus side scatter (SSC-A) on the y-axis. A rectangular gate, labeled "P2" (2.48%), isolates the population of CD235-positive cells.

Panel C (Bottom Left): CD235 FITC-A vs. TRAPPC4 PE-A (P2 Gated): This plot presents CD235 expression (FITC-A) against TRAPPC4 fluorescence (PE-A) for the P2 gated population. Events are quadranted to identify distinct populations. Q1-LR (98.84%) represents cells that are CD235-positive and TRAPPC4-negative, while Q1-UR (1.16%) corresponds to a small subset of cells co-expressing both markers.

Panel D (Bottom Right): CD235 FITC-A vs. FTL PerCP-A (P2 Gated): In this plot, CD235 expression (FITC-A) is shown against FTL fluorescence (PerCP-A) for the P2 gated population. The majority of events fall in Q2-LR (100.00%), which corresponds to cells that are CD235-positive and FTL-negative. A small population (Q2-UR, 0.00%) represents cells that co-express both markers.

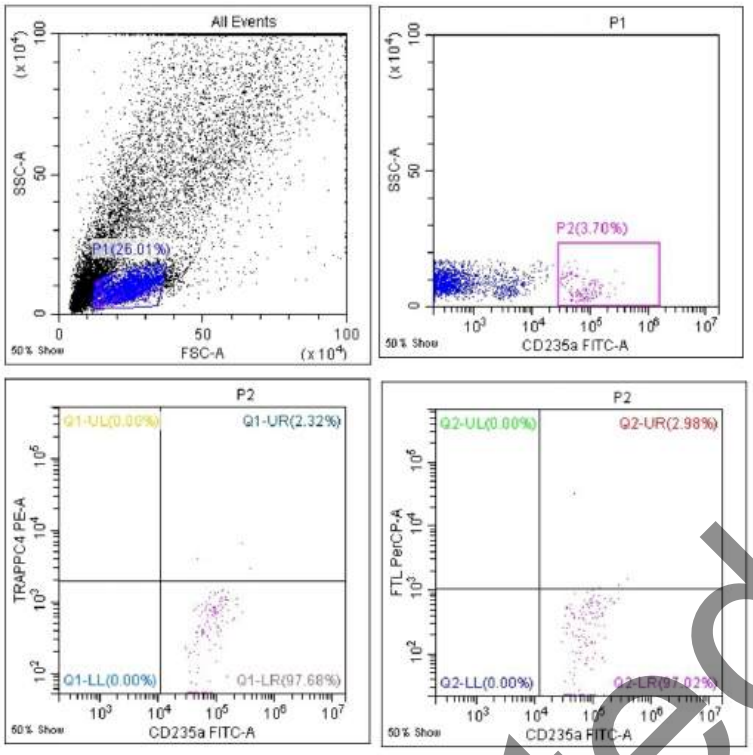

Figure S1f: CD235 IRP

Panel A (Top Left): FSC-A vs. SSC-A (All Events): This scatter plot shows the distribution of all events based on forward scatter (FSC-A) and side scatter (SSC-A), indicating cell size and granularity. The gated population, labeled "P1," comprises 26.01% of the total events.

Panel B (Top Right): CD235 FITC-A vs. SSC-A (P1 Gated): This plot shows CD235 expression (FITC-A) on the x-axis versus side scatter (SSC-A) on the y-axis for the P1 gated population. The gate "P2" (3.70%) isolates the CD235-positive population.

Panel C (Bottom Left): CD235 FITC-A vs. TRAPPC4 PE-A (P2 Gated): This plot presents CD235 expression (FITC-A) against TRAPPC4 fluorescence (PE-A) for the P2 gated population. Quadrant analysis shows Q1-LR (97.68%) with high CD235 and low TRAPPC4 expression, and Q1-UR (2.32%) as a minor population expressing both markers.
Panel D (Bottom Right): CD235 FITC-A vs. FTL PerCP-A (P2 Gated): In this plot, CD235 expression (FITC-A) is shown against FTL fluorescence (PerCP-A) for the P2 gated population. The majority of events fall in Q2-LR (97.02%) with high CD235 and low FTL expression, while Q2-UR (2.98%) represents a small population co-expressing both markers.